

1 SUPPLEMENTARY MATERIAL FOR:
2 CORRELATION BETWEEN TECTONIC STRESS
3 REGIMES AND METHANE SEEPAGE ON THE WEST-
4 SVALBARD MARGIN

5 **Andreia Plaza-Faverola¹ and Marie Keiding²**

6 ¹ *CAGE-Centre for Arctic Gas Hydrate, Environment, and Climate; Department of Geology,*
7 *UiT The Arctic University of Norway, N-9037 Tromsø, Norway*

8 ² *Geological Survey of Norway (NGU), P.O. Box 6315 Sluppen, 7491 Trondheim, Norway*

9

10 **Tectonic model parameters**

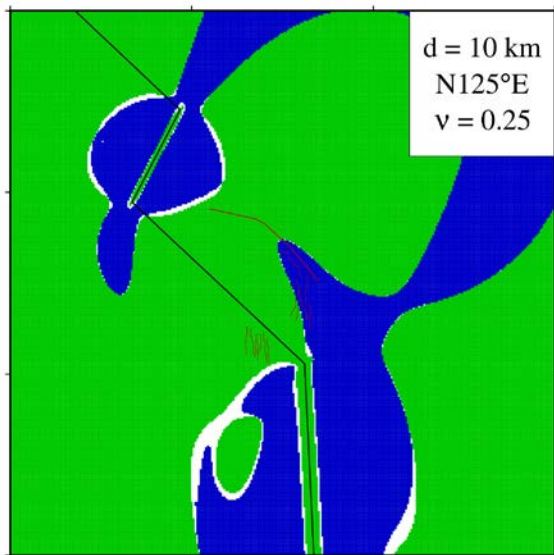
Table 1. Model parameters for the two rectangular planes (Okada, 1985) used to approximate the deformation due to oblique spreading along Molloy Ridge (MR) and Knipovich Ridge (KR)										
Ridge	Length (km)	Depth to lower boundary (km)	Depth upper boundary (km)	Dip (°)	Strike (°)	East midpoint (UTM, m)	North midpoint (UTM, m)	Right-lateral motion* (mm/yr)	Vertical motion (mm/yr)	Opening* (mm/yr)
MR	57	900	10	-90	28	380.000	8820.000	1.8	0	13.9
KR	180	900	10	-90	-3	467.000	8616.000	8.6	0	11.1

* Calculated by assuming a half spreading rate of 7 mm/yr in the direction of N125°E on both the MR and KR.

11

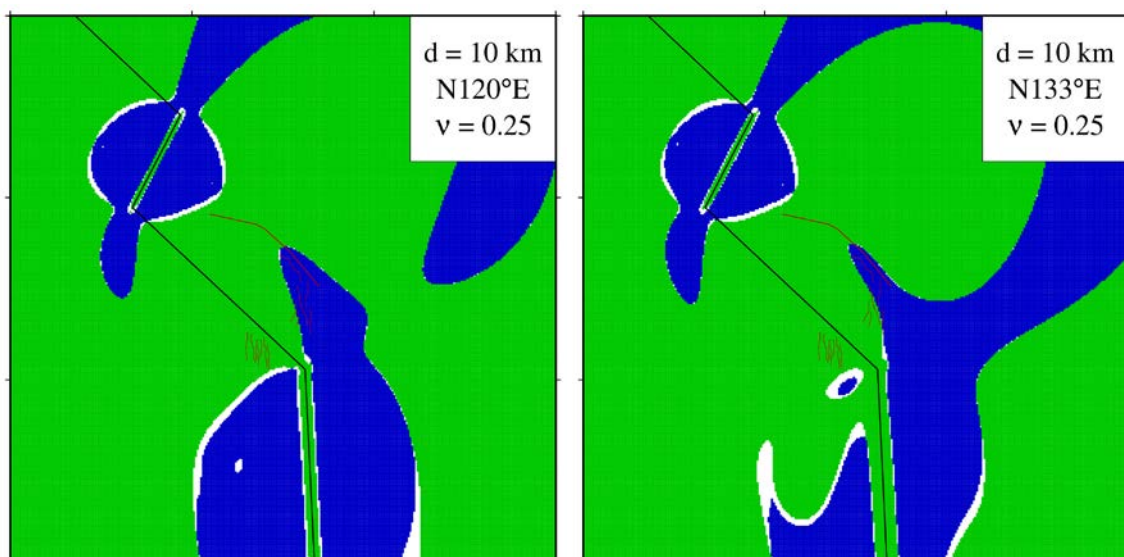
12 **Sensitivity tests**

13 To test the robustness of the modelling, in particular with respect to the change from tensile stress on
14 the eastern Vestnesa Ridge (VR) to strike-slip stress along the western VR, we examine the influence
15 of varying the following model parameters: spreading along the Molloy Ridge (MR) and the Knipovich
16 (KR), depth of brittle-ductile transformation (upper boundary of planes), and elastic moduli (Poisson's
17 ratio and shear modulus).



27 **Fig. S1:** Our preferred model with depth, $d = 10$ km to the upper boundary of the dislocations, a
 28 spreading direction of $N125^\circ E$ and a Poisson's ratio $\nu = 0.25$. Green = strike-slip stress, blue = tensile
 29 stress, red = compressive stress regime. The crest of Vestnesa ridge and faults are marked with thin red
 30 lines.

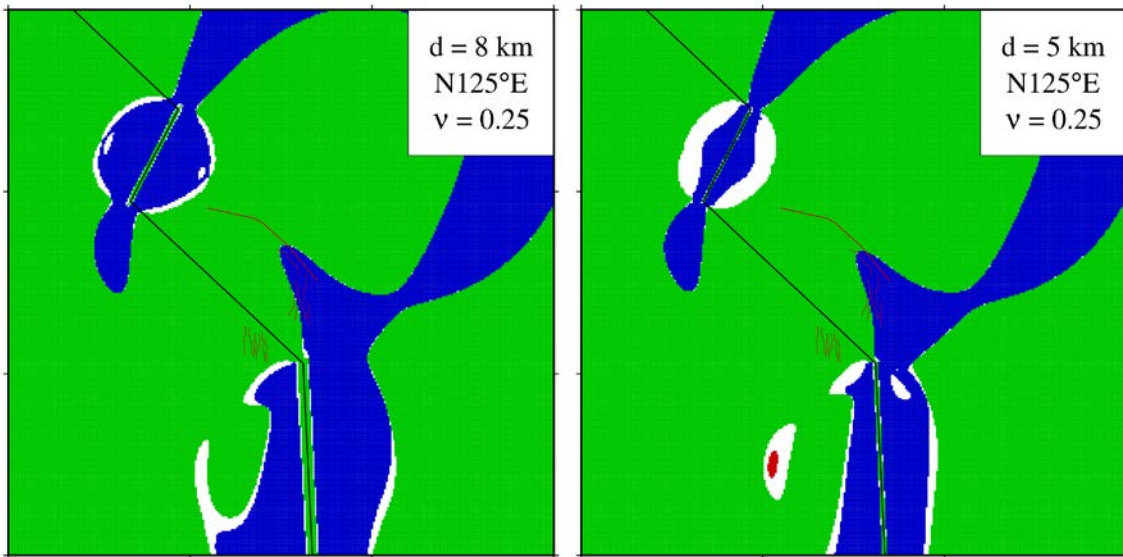
31 **Spreading along MR and KR:** We used a spreading direction of $N125^\circ E$ along the Molloy Ridge (MR)
 32 and the northern part of the Knipovich Ridge (KR) from recent plate motion models by Altamimi et al.,
 33 (2002), Argus et al., (2010), and DeMets et al., (2010). Other recent plate models give slightly different
 34 spreading directions, i.e. $N120^\circ E$ (Drewes, 2009) or $N133^\circ E$ (Kreemer et al., 2014). The direction of
 35 $N133^\circ E$ is parallel to the trend of the Molloy Transform Fault (MTF). The use of these alternative
 36 spreading directions would either broaden or reduce the zone of tensile stress at eastern VR, however,
 37 the zone is still present also with a spreading direction of $N133^\circ E$ (Fig. S2). Changing the spreading rate
 38 would only affect the magnitude of the predicted stresses, which are not considered in the present study.



39
 40 **Fig. S2:** Varying the spreading direction.

41 **Depth to upper boundary (i.e., the depth of the brittle-ductile transition in the model):** The actual
 42 depth is not well constrained in the study area, but farther south along the Atlantic Ocean, Keiding et al.

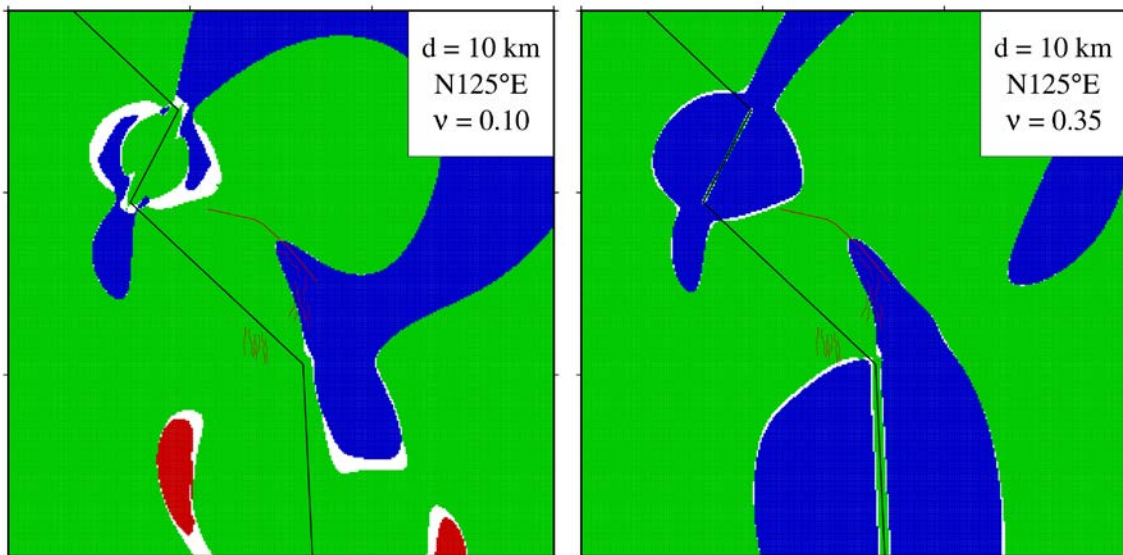
43 (2008) estimated the depth along part of the Mid-Atlantic plate boundary in Iceland to be 6-7 km using
44 the same modelling technique and constraint from GPS observations. Hence, the 10 km used in our
45 models may be on the deeper side. Changing the depth to more shallow values, decreases the zone of
46 tensile stress at eastern VR, but it is still apparent with an upper boundary depth of 5 km (Fig. S2).



47

48 Fig. S3: Reducing the depth to upper boundary of dislocation.

49 **Elastic moduli:** The typical range of Poisson's ratio for rocks is 0.1-0.35 (e.g., Gercek, 2007). Varying
50 the Poisson's ration within this range results in markedly different stress patterns to the sides of the
51 spreading ridges, however, the zone of tensile stress at eastern VR remains almost unaltered (Fig. S4).
52 Varying the shear modulus will only affect the magnitude of the predicted stresses, which are not
53 considered in the present study.



54

55 Fig. S4: Varying Poisson's ratio.

56 **References:**

57 Altamimi, Z., Sillard, P., and Boucher, C., 2002, ITRF2000: A new release of the International Terrestrial
58 Reference Frame for earth science applications: *Journal of Geophysical Research: Solid Earth*,
59 v. 107, no. B10, p. ETG 2-1-ETG 2-19.

60 Argus, D. F., Gordon, R. G., Heflin, M. B., Ma, C., Eanes, R. J., Willis, P., Peltier, W. R., and Owen, S. E.,
61 2010, The angular velocities of the plates and the velocity of Earth's centre from space
62 geodesy: *Geophysical Journal International*, v. 180, no. 3, p. 913-960.

63 DeMets, C., Gordon, R. G., and Argus, D. F., 2010, Geologically current plate motions: *Geophysical*
64 *Journal International*, v. 181, no. 1, p. 1-80.

65 Drewes, H., 2009, The Actual Plate Kinematic and Crustal Deformation Model APKIM2005 as Basis for
66 a Non-Rotating ITRF, *in* Drewes, H., ed., *Geodetic Reference Frames: IAG Symposium Munich*,
67 *Germany, 9-14 October 2006: Berlin, Heidelberg, Springer Berlin Heidelberg*, p. 95-99.

68 Gercek, H., 2007, Poisson's ratio values for rocks: *International Journal of Rock Mechanics and Mining*
69 *Sciences*, v. 44, no. 1, p. 1-13.

70 Keiding, M., Árnadóttir, T., Sturkell, E., Geirsson, H., and Lund, B., 2008, Strain accumulation along an
71 oblique plate boundary: the Reykjanes Peninsula, southwest Iceland: *Geophysical Journal*
72 *International*, v. 172, no. 2, p. 861-872.

73 Kreemer, C., Blewitt, G., and Klein, E. C., 2014, A geodetic plate motion and Global Strain Rate Model:
74 *Geochemistry, Geophysics, Geosystems*, v. 15, no. 10, p. 3849-3889.

75 Okada, Y., 1985, Surface deformation due to shear and tensile faults in a half-space: *Bulletin of the*
76 *Seismological Society of America*, v. 75, no. 4, p. 1135-1154.

77

78